ACS Infectious Diseases

pubs.acs.org/journal/aidcbc

Article

Unique Cell Surface Mannan of Yeast Pathogen *Candida auris* with Selective Binding to IgG

Lufeng Yan,[#] Ke Xia,[#] Yanlei Yu, Anna Miliakos, Sudha Chaturvedi, Fuming Zhang, Shiguo Chen, Vishnu Chaturvedi,[*] and Robert J. Linhardt[*]

Cite This: *ACS Infect. Dis.* 2020, 6, 1018−1031

Read Online

ACCESS | Metrics & More | Article Recommendations | Supporting Information

ABSTRACT: The emerging, multidrug-resistant yeast pathogen *Candida auris* is responsible for healthcare-associated outbreaks across the globe with high mortality. The rapid spread of *C. auris* is linked to its successful colonization of human skin, followed by bloodstream infections. We compared glycomics and proteomics of *C. auris* to closely and distantly related human pathogenic yeasts, *C. haemulonii* and *C. albicans*, with the aim to understand the role of cell surface molecules in skin colonization and immune system interactions. *Candida auris* mannan is distinct from other pathogenic *Candida* species, as it is highly enriched in β-1,2-linkages. The experimental data showed that *C. auris* surface mannan β-1,2-linkages were important for the interactions with the immune protein IgG, found in blood and in sweat glands, and with the mannose binding lectin, found in the blood. *Candida auris* mannan binding to IgG was from 12- to 20-fold stronger than mannan from the more common pathogen *C. albicans*. The findings suggest unique *C. auris* mannan could be crucial for the biology and pathogenesis of this emerging pathogen.

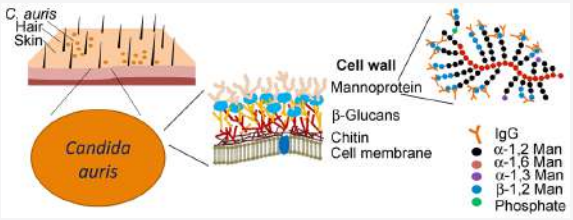

KEYWORDS: *Candida auris, glycomics, proteomics, mannan, adhesion, immunoglobin*

Candida auris is an emerging multidrug-resistant (MDR) yeast that can cause a systemic infection leading to death.[1−7] Over the past years, there has been a surge of nearly 1,000 cases in the US, particularly in the New York metropolitan area.[4,7,8] *C. auris* can colonize the skin, ears (hence the designation "auris"[1]), and other body sites where it remains asymptomatic.[6−8] The problem comes when *C. auris* moves into the body through a wound, sore, or puncture leading to systemic infection and the death of nearly half of those infected.[6,7,9]

Strikingly, *C. auris* colonization of the human skin is difficult to eradicate despite chlorhexidine bathing, and the unusual persistence of the pathogen on inanimate objects in hospitals and nursing homes requires the use of bleach as the disinfectant.[8,10−13] On the skin, *C. auris* binds tightly, displacing many other organisms typically comprising a healthy microbiome, is difficult to remove even using soap, alcohol, and iodine disinfectants, and is easily transmissible between patients.[8] Once inside the body, it is unclear what proteins/tissues interact with *C. auris*. There is a lack of mechanistic insight into the adherence properties of *C. auris*, and despite the availability of several whole genomes, structural elements underlying adhesion remain unknown in the absence of a fully annotated genome.[2,5,12]

The external surface of pathogenic yeasts, comprising the cell wall, is over 60% carbohydrate and is essential to nearly every aspect of the biology and pathogenicity.[14] Cell wall mannoproteins are composed of *N*- and *O*-linked mannans with α-1,2-, α-1,3-, α-1,6- and β-1,2-linked mannopyranose residues as well as phospho-linked mannopyranose units.[15] These mannoproteins are potent immunogens that trigger and modulate the host innate immune response through DC-SIGN (dendritic cell specific intracellular adhesion molecule-3 (ICAM-3) grabbing nonintegrin), mannose receptor, and Dectin-2[16] during candidiasis.[14] Mannoproteins are adhesins (mannans with lectin-like properties[17,18]) and promote *Candida* binding to endothelial and epithelial cells.[19−22] Different *Candida* species have different glycan structures.[15] *Candida* mannans and mannoproteins are highly immunogenic and effective vaccines in animal models of candidiasis.[23−25] Fungal mannan antigenemia is also regarded as a diagnostic indicator of invasive *Candida* infections.[26,27] At present, we know little about the cell wall, the mannoproteins, mannans, and the glycome of *C. auris*.

We describe a comparative study of the cell wall glycome and proteome of *C. auris* and closely and distantly related yeast pathogens, *C. haemulonii* and *C. albicans*. Our data show a unique structure of *C. auris* mannan and an ability to bind IgG.

Received: November 21, 2019
Published: April 1, 2020

https://dx.doi.org/10.1021/acsinfecdis.9b00450
ACS Infect. Dis. 2020, 6, 1018−1031

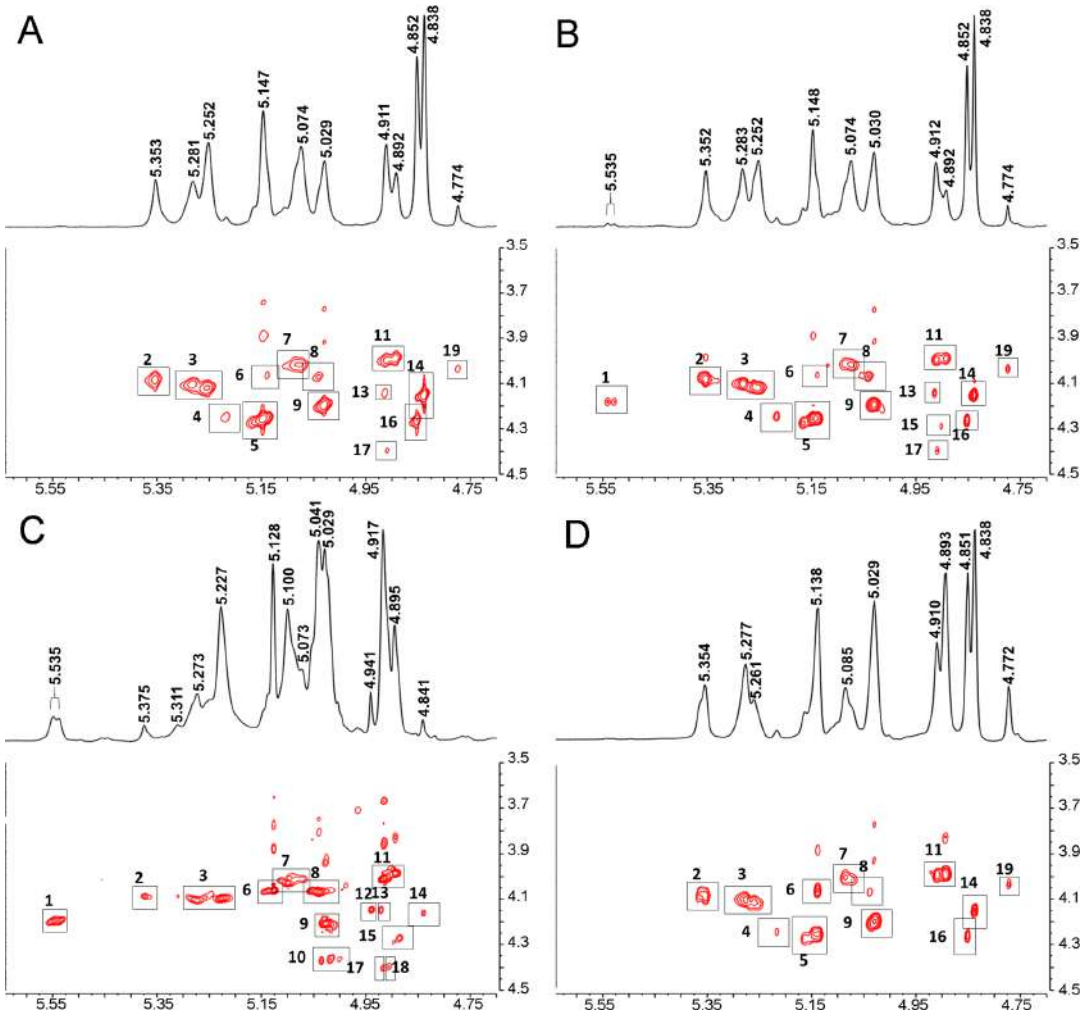

Figure 1. TOCSY spectra of *Candida* mannans. (A) *C. auris* 16-4 mannan; (B) *C. auris* 17-12 mannan; (C) *C. albicans* mannan; (D) *C. haemulonii* mannan. The boxed regions in each spectrum indicate the H-1−H-2-correlated cross-peaks of the α- and β-mannose residues in each whole mannan. Shift values are in ppm.

RESULTS

Prediction of the Structure of the Four Mannans Using Total Correlation Spectroscopy (TOCSY). We compared the structures of the four *Candida* mannans using their TOCSY spectra. The H-1 region (4.70−5.65 ppm) of the one-dimensional (1D) NMR spectra and the 2D-H-1−H-2-correlated cross-peaks of the four mannans are shown in Figure 1. The mannans from the two *C. auris* strains showed almost the same H-1 region, giving relatively simple signals in the α-anomeric region (about 4.90−5.40 ppm) and obvious signals at the β-anomeric region (about 4.70−4.90 ppm) as described in previous reports on mannan structure.[15] The *C. haemulonii* mannan showed a similar H-1 region as the two *C. auris* mannans, but it showed less intense β-anomeric region signals. The *C. albicans* mannan gave only complex signals in the α-anomeric region, suggesting a mannan very different from that of *C. auris*. Clearly observed signals at 5.54 ppm of the H-1 region of *C. albicans* mannan and *C. auris* strain 17-12 mannan indicate both have a considerable number of phosphodiesterified oligosaccharides.[28] More detailed structural differences among the four mannans were apparent in the TOCSY spectra on the basis of the previously published assignments of *C. albicans*, *C. lusitaniae*, *C. parapsilosis*, and *C. guilliermondii* mannans.[15,28−31] The differences between cross-peaks 3 and 8 (Figure 1), which correspond to α-1,2-linked mannose units in the mannans, suggest differences in the lengths of the α-1,2-linked side-chain moieties. Compared to the *C. albicans* mannan, the other three *Candida*-derived mannans contained greater amounts of one or two β-1,2-linked mannose units at the terminal of the side-chain moieties, reflected by the cross-peaks 4, 5, 14, 16, and 19 (Figure 1). However, the cross-peaks 10, 12, and 18, which correspond to four or more mannose units of the β-1,2-linked chain, only appear in *C. albicans* mannan. Cross-peak 6, corresponding to the terminal α-1,3-linked mannose units of the mannans, was more obvious in *C. albicans* mannan and *C. haemulonii* mannan than in the mannans from the two *C. auris* strains.

Analysis of Phosphodiesterified Oligosaccharides. We next used mild acid conditions to treat the four mannans and then used centrifugal filter units to collect acid-labile

https://dx.doi.org/10.1021/acsinfecdis.9b00450
ACS Infect. Dis. 2020, 6, 1018−1031

oligosaccharides to determine the yield and structure of the phosphodiesterified oligosaccharides. In the high performance gel permeation chromatography (HPGPC) profiles of the acid-labile oligosaccharides, the 34 to 46 min range showed the phosphodiesterified oligosaccharides (Figure 2A). We identified the chain sizes for these peaks of 1 to 7 saccharide units. Since monosaccharides are easily lost from these polysaccharides under acidic conditions, only a small portion of monosaccharides is likely phosphodiesterified. The phosphodiesterified oligosaccharides of *C. albicans* mannan are rich in mannotriose to mannoheptaose, while those of the other three mannans were comprised predominantly of mannotriose. We next separated phosphodiesterified oligosaccharides (≥ mannotriose) for further analysis. From these analyses, the yields of *C. auris* 16-4 mannan, *C. auris* 17-12 mannan, *C. albicans* mannan, and *C. haemulonii* mannan were estimated to be 0.9%, 2.1%, 7.6%, and 1.1%, respectively. The H-1 regions of the ^{1}H NMR spectra of four sources of phosphodiesterified oligosaccharides (≥ mannotriose) are shown in Figure 2B. On the basis of the assignments of the H-1 signals, the structures of the phosphodiesterified oligosaccharides (≥ mannotriose) from *C. albicans* mannan include β-1,2-linked mannotriose to mannoheptaose. The phosphodiesterified oligosaccharides (≥ mannotriose) from the two *C. auris* mannans and *C. haemulonii* mannan have the same, relatively simple structure that was identified as β-1,2-linked mannotriose. Their H-1 proton chemical shifts are shown in Table S1.

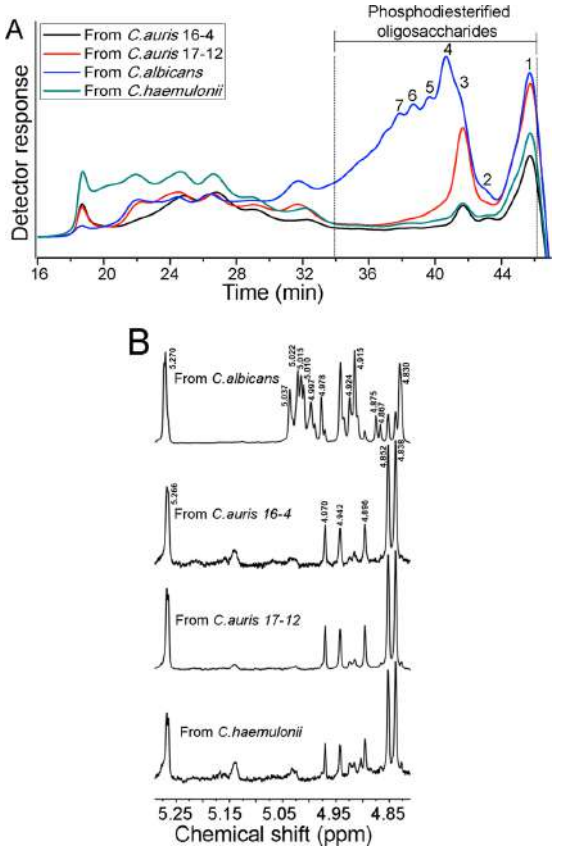

Figure 2. Analysis of acid labile oligosaccharides from the four *Candida* mannons. (A) HPGPC profiles of acid-labile oligosaccharides from four mannans by a Superdex Peptide 10/300 GL column. Numbers 1 to 7 indicate the relative positions of mannose to mannoheptaose. (B) The H-1 region of the ^{1}H NMR spectra of four sources of phosphodiesterified oligosaccharides (≥ mannotriose).

Acetolysis of the Acid-Stable Portions of the Four Mannans. The acetolysis results profiled by HPGPC are shown in Figure 3A. The larger molecular size (> mannooctaose) portions indicate that the acetolysis degradation was not excessive.

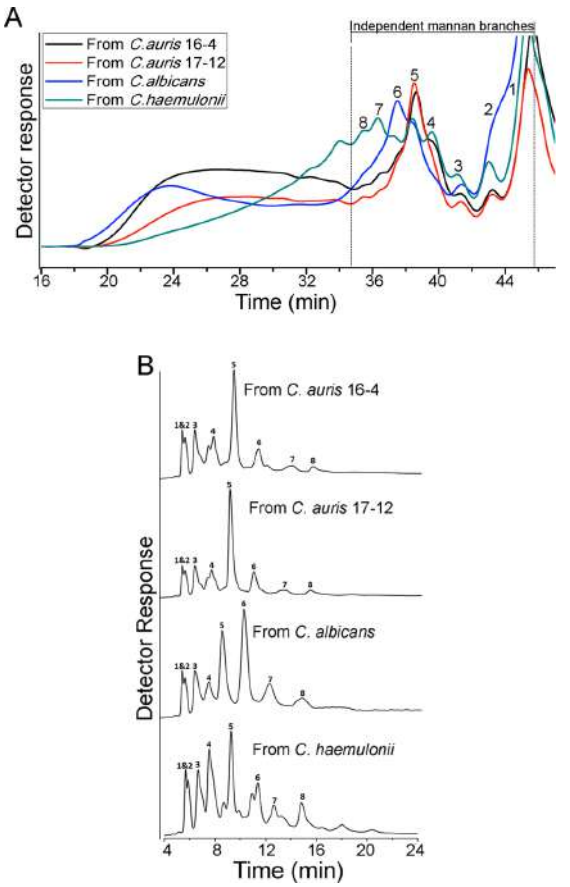

Figure 3. HPGPC and HPLC of acid-stable mannan branches. (A) HPGPC profiles of acetolysis result in oligosaccharides from four mannans by a Superdex Peptide 10/300 GL column. Numbers 1 to 8 indicate the relative positions of mannose to mannooctaose. (B) HPLC elution patterns of aimed independent branch oligosaccharides from four mannans by a YMC Pack PA-G column. Numbers 1 to 8 indicate the relative positions of mannose to mannooctaose, and they were judged according to the correspondence between HPGPC and HPLC profiles of eight oligosaccharide fractions from *C. auris* 16-4 as shown in Figure S2.

Oligosaccharides from mannose to mannooctaose represent independent branches of the *Candida* mannans on the basis of previous reports.[15,28] The two *C. auris* mannans show a similar distribution of different size branches, in which mannopentaose is the major branch compound. For *C. albicans* mannan, the mannohexaose is the major branch component. However, *C. haemulonii* mannan had similar amounts of branches from

https://dx.doi.org/10.1021/acsinfecdis.9b00450
ACS Infect. Dis. 2020, 6, 1018−1031

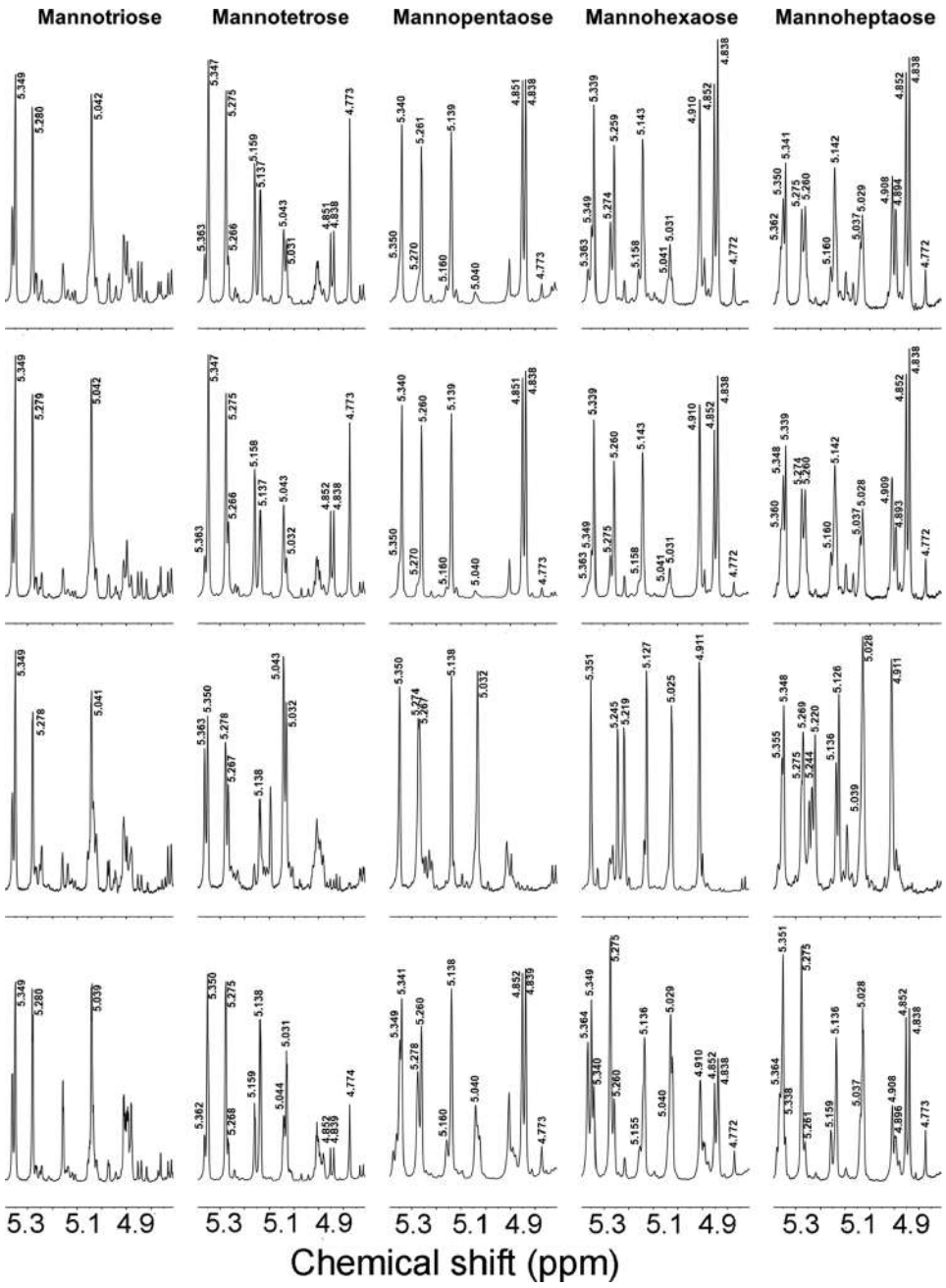

Figure 4. ^{1}H NMR spectral data on *Candida* mannans. Anomeric region of the ^{1}H NMR spectra of oligosaccharides (shift values in ppm) from (A) *C. auris* 16-4 mannan; (B) *C. auris* 17-12 mannan; (C) *C. albicans* mannan; (D) *C. haemulonii* mannan obtained by acetolysis.

mannotetrose to mannooctaose. We next size-separated oligosaccharides, mannose to mannooctaose, obtained by acetolysis for further structural analysis (Figure S1). These were next eluted by high performance liquid chromatography (HPLC) from a YMC Pack PA-G column, as shown in Figure 3B for optimal separation of different size branches. Each size of oligosaccharide was, thus, obtained for further NMR analysis.

NMR Analysis of Branched Oligosaccharides. The H-1 regions of the ^{1}H NMR spectra of branched oligosaccharides from four mannans, including from mannotriose to mannoheptaose, are shown in Figure 4. Structural analyses of mannooctaoses are not shown, as they have similar structural features of the smaller oligosaccharides and are secondary in amounts of these mannans. Consistent with NMR spectra of the mannan polysaccharides, each size of branched oligosaccharides from two *C. auris* mannans showed almost the same NMR spectra. In addition, signals corresponding to the one or two β-1,2-linkages, at about 4.77 or 4.84 and 4.85 ppm,[28,29] were present in branched oligosaccharides from the two

https://dx.doi.org/10.1021/acsinfecdis.9b00450
ACS Infect. Dis. 2020, 6, 1018−1031

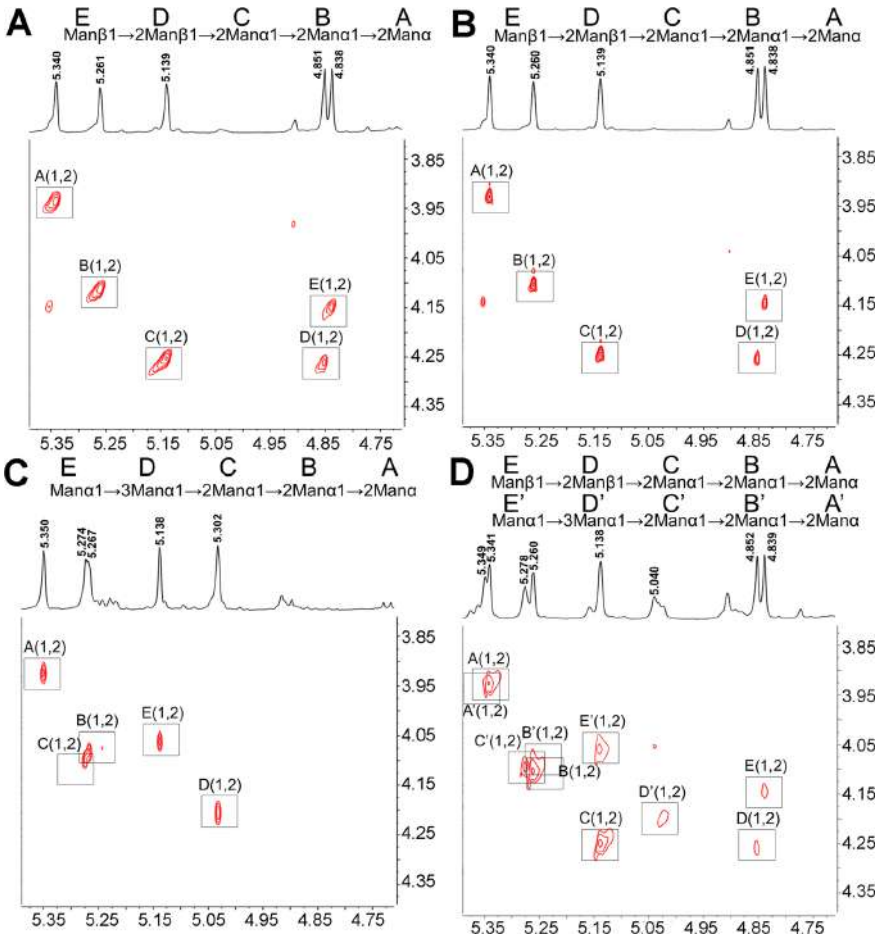

Figure 5. TOCSY spectra with H-1−H-2-correlated cross-peaks assignments in ppm of mannopentaose from (A) *C. auris* 16-4 mannan; (B) *C. auris* 17-12 mannan; (C) *C. albicans* mannan; (D) *C. haemulonii* mannan.

C. auris mannans, including from mannotetrose to mannoheptaose. Branched oligosaccharides from *C. haemulonii* mannan also had weaker signals corresponding to one or two β-1,2-linkages. However, the branched oligosaccharides from *C. albicans* mannan showed almost no β-1,2-linkages. From the following, according to previous reports about the structure of *Candida* branch oligosaccharides, we can establish the structures of each branched oligosaccharide from four mannan sources and provide their H-1 assignments in Table S2.

The H-1 regions of the ^{1}H NMR spectra of the mannotriose of the mannans from the four *Candida* sources are similar except for some signals from unavoidable mannotriose impurities, and most of the signals at about 5.04, 5.28, and 5.35 ppm could be easily assigned as the H-1 of Manα1-2Manα1−2Manα.[29] This structure is the basis for all extensions of branched oligosaccharides from the acid-labile portion of the four *Candida* mannans.

The H-1 regions of the ^{1}H NMR spectra of mannotetrose show some differences among the four sources of mannans. The most obvious structure for mannotetrose from the two *C. auris* mannans is Manβ1-2Manα1-2Manα1-2Manα, on the basis of the assignments of H-1 at 4.77, 5.16, 5.28, and 5.35 ppm.[29] In addition, we observed similar amounts of Manα1-2Manα1-2Manα1-2Manα, Manα1-3Manα1-2Manα1-2Manα, and Manβ1-2Manβ1-2Manα1-2Manα according to their NMR spectra.[28,30,31] The mannotetrose structure from *C. albicans* mannan showed similar amounts of Manα1-2Manα1-2Manα1-2Manα and Manα1-3Manα1-2Manα1-2Manα. Mannotetrose from *C. haemulonii* mannan had the same four structures as those from *C. auris* mannans, but its majority was Manα1-3Manα1-2Manα1-2Manα according to the specific signal at 5.03 ppm, and Manβ1-2Manβ1-2Manα1-2Manα was only present in small amounts.

Mannopentaose occupied the most significant portion of all the branched oligosaccharides for four sources of mannans as shown by HPGPC and HPLC profiles. Thus, we performed TOCSY to obtain a definitive structural assignment (Figure 5). The mannopentaose from *C. auris* mannans gave simple signals for 2D-H-1−H-2-correlated cross-peaks, which could be assigned as Manβ1-2Manβ1-2Manα1-2Manα1-2Manα.[28,29] In addition, mannopentaose from *C. auris* mannans showed small amounts of Manα1-3Manα1-2Manα1-2Manα1-2Manα[30] and Manβ1-2Manα1-2Manα1-2Manα1-2Manα[28] structures. The TOCSY spectrum of mannopentaose from *C. albicans* mannan could be assigned as Manα1-3Manα1-2Manβ1-2Manα1-2Manα. However, mannopentaose from *C. haemulonii* mannan contained similar amounts of Manβ1-2Manβ1-2Manα1-

https://dx.doi.org/10.1021/acsinfecdis.9b00450
ACS Infect. Dis. 2020, 6, 1018−1031

2Manα1-2Manα and Manα1-3Manα1-2Manα1-2Manα1-2Manα as major structures and a small amount of Manβ1-2Manα1-2Manα1-2Manα1-2Manα.

Mannohexaose of *C. auris* mannans contained a major structure with two β-1,2-linkages at the nonreducing terminal as suggested by the signals at 4.84 and 4.85 ppm. The signal intensity at 4.84 ppm, however, was not equal to the signal intensity at 4.85 ppm, as shown in the ^{1}H NMR spectra. When the remarkable signal at 4.91 ppm and the major signal at 4.84 ppm were combined, the structure of three β-1,2-linkages at the nonreducing terminal could be inferred.[28,29] In addition, we also inferred minor structures corresponding to Manβ1-2Manα1-2Manα1-2Manα1-2Manα1-2Manα and Manα1-2Manα1-3Manα1-2Manα1-2Manα. The mannohexaose structure of *C. albicans* mannan was established as Manα1-3(Manα1-6)Manα1-2Manα1-2Manα1-2Manα.[30]

The mannohexaose structures of *C. haemulonii* mannan showed the same four structures as the mannohexaose obtained from *C. auris* mannan. However, the structures with two or three β-1,2-linkages at the nonreducing terminal were of significantly less abundance, and the Manα1-2Manα1-3Manα1-2Manα1-2Manα1-2Manα was the major structure.

The mannoheptaose component of the *C. auris* mannans followed the style of mannohexaose, which contained the one, two, or three β-1,2-linkages at the nonreducing terminal, and the structures containing two β-1,2-linkages were predominant. There were no mannans with four or more β-1,2-linkages at the nonreducing terminal, since there were no signals at 4.93 ± 0.01 ppm.[28] In addition in the *C. auris* mannans, we also found appreciable quantities of Manα1-2Manα1-3Manα1-2Manα1-2Manα1-2Manα with a α-1,6-linkage at the reducing terminal in mannoheptaose. The α-1,6-linkage at the reducing terminal is believed to be the result of incomplete acetolysis. The α-1,6-linkage did not add to the latter mannose of the α-1,3-linkage, because there were no signals at about 5.22 and 5.24 ppm.[30] The mannoheptaose structure of *C. albicans* mannan could be established as Manα1-2Manα1-3Manα1-2Manα1-2Manα1-2Manα with a α-1,6-linkage at the reducing terminus or the latter mannose with a α-1,3-linkage. The mannohexaose structures of *C. haemulonii* mannan showed the same four structures as *C. auris* mannan mannohexaose, with the Manα1-2Manα1-3Manα1-2Manα1-2(Manα1-6)Manα being the major structure.

Identification of *C. auris* Cell Surface Binding Proteins from Human Serum. Human serum from a pool of healthy donor volunteers was incubated with *C. auris* strains 16-4 and 17-12, respectively, and each strain had a duplicate incubation sample. Incubated cells were washed with Tween 20 to remove nonspecific weak-binding proteins on the surface. Strong-binding proteins on cell surfaces were digested by trypsin with the help of reducing agent dithiothreitol (DTT) for deep digestion. Digested peptides were then separated from cells and processed for proteomics identification.

Proteomic analyses of human serum proteins binding to *C. auris* were performed with replicate MS runs for each sample. The significant proteins having a false discovery rate (FDR) of <1% are shown in Table 1. Each protein listed had more than two identified peptides. There were 13 common proteins found in the *C. auris* 16-4 replicates and 15 common proteins found in the *C. auris* 17-12 replicates (Table 1). There were 8 proteins shared by the two *C. auris* strains (bold font in Table 1), including three keratins that are routinely viewed as contaminants in proteomic analyses. The five other proteins identified were tested using surface plasmon resonance (SPR) for their interaction with the four *Candida* mannans.

Table 1. Proteins Identified in *C. auris* Binding by Proteomics Analysis

proteins from *C. auris* 16-4	proteins from *C. auris* 17-12
complement C3	**complement C3**
immunoglobulin heavy constant gamma	**immunoglobulin heavy constant gamma**
histidine-rich glycoprotein	**histidine-rich glycoprotein**
mannose-binding protein C	**mannose-binding protein C**
apolipoprotein A-I	**apolipoprotein A-I**
keratin, type II cytoskeletal 1	**keratin, type II cytoskeletal 1**
keratin, type I cytoskeletal 9	**keratin, type I cytoskeletal 9**
keratin, type I cytoskeletal 10	**keratin, type I cytoskeletal 10**
complement C1q subcomponent subunit A	plasminogen
prothrombin	apolipoprotein C-III
T cell receptor alpha joining 56	cotranscriptional regulator FAM172A
protein phosphatase 1 regulatory subunit 26	apolipoprotein B-100
complement C1q subcomponent subunit C	inter-alpha-trypsin inhibitor heavy chain H2
	alpha-1-antitrypsin
	apolipoprotein C-I

Interaction Studies between *Candida* Mannans and Serum Proteins. We tested the interactions of the five serum proteins, complement C3, IgG, human histidine-rich glycoprotein (HPRG), apolipoprotein A-I, and human mannan binding lectin (MBL) protein, with the surface *C. auris* cells to understand what factors might play a role in the systemic *C. auris* infections. We discovered that only IgG and MBL protein showed strong binding to all four mannans. Their interaction kinetic constants are shown in Table 2, and the sensorgrams with a fitted curve are shown in Figure S3. IgG, the most common type of antibody in the blood,[32] showed the strongest interaction to the two *C. auris* mannans and exhibited similar K_D values (Table 2). *C. haemulonii* mannan showed a weaker interaction with IgG, and *C. albicans* mannan showed the weakest interaction with IgG. MBL protein is instrumental in innate immunity[33] and showed a stronger interaction with four sources of mannans than did IgG. Moreover, MBL is known to specifically bind to D-mannose residues found on the surfaces of many pathogens and showed the strongest interactions for mannans rich in β-1,2-linkages (Table 2).

We used these four mannans to compete with the binding between IgG and immobilized *C. auris* 16-4 mannan to further compare the interaction strength between IgG and four mannans (Figure 6). We found that, at the same IgG concentration (1 μM), only 0.14 μM *C. auris* 16-4 mannan could reduce by half the amount of IgG interacting with immobilized *C. auris* 16-4 mannan. However, for *C. albicans* mannan, the concentration required 1.70 μM to reduce by half the amount of IgG interacting with immobilized *C. auris* 16-4 mannan. The concentrations of *C. auris* 17-12 mannan and *C. haemulonii* mannan required to achieve the same competitive inhibition were 0.19 and 0.27 μM, respectively. These competition results also suggest that the *C. auris* mannan with a higher content of β-1,2-linked mannose residues showed a stronger binding for IgG.

Cell Surface Mannoproteins. Cell surface mannoproteins were isolated as shown in Figure 7. In this isolation process, the yeast cells remained intact (Figure S4).

https://dx.doi.org/10.1021/acsinfecdis.9b00450
ACS Infect. Dis. 2020, 6, 1018−1031

Table 2. Kinetic Constants of Interactions between Immune Protein and Four Sources of Mannans[a]

protein	mannan	k_a (1/Ms)	k_d (1/s)	K_D (M)
IgG	*C. auris* 16-4 mannan	853 ± 25.3	$4.04 \times 10^{-4} \pm 6.58 \times 10^{-6}$	4.73×10^{-7}
	C. auris 17-12 mannan	$2.83 \times 10^{3} \pm 127$	$1.52 \times 10^{-3} \pm 1.46 \times 10^{-5}$	5.37×10^{-7}
	C. albicans mannan	286 ± 17.6	$3.04 \times 10^{-3} \pm 3.42 \times 10^{-5}$	1.06×10^{-5}
	C. haemulonii mannan	488 ± 38.7	$7.88 \times 10^{-4} \pm 1.33 \times 10^{-5}$	1.61×10^{-6}
MBL protein	*C. auris* 16-4 mannan	$1.35 \times 10^{5} \pm 1.06 \times 10^{3}$	$1.05 \times 10^{-7} \pm 1.06 \times 10^{-6}$	7.81×10^{-13}
	C. auris 17-12 mannan	$1.31 \times 10^{5} \pm 1.58 \times 10^{3}$	$1.31 \times 10^{-7} \pm 1.00 \times 10^{-6}$	1.00×10^{-12}
	C. albicans mannan	$6.68 \times 10^{4} \pm 716$	$1.56 \times 10^{-5} \pm 1.64 \times 10^{-5}$	2.34×10^{-10}
	C. haemulonii mannan	$5.24 \times 10^{4} \pm 592$	$4.01 \times 10^{-7} \pm 5.36 \times 10^{-6}$	7.65×10^{-12}

[a]The standard errors are from the global fitting.

A summary of the common identified proteins with predicted functions is presented in Table S3. These proteins were identified with high confidence (FDR < 0.01), and each was hit by at least two peptides in both biological samples, *C. auris* 16-4 and 17-12. Most proteins were described as "uncharacterized" due to the poorly annotated *C. auris* proteome. Further functional predictions and annotations were carried out on the basis of Uniprot[36] and Pannzer2.[37] There were 96 proteins initially identified, but due to the poorly annotated *C. auris* proteome, many of these were uncharacterized proteins; only 63 had a protein description or predicted function (Table S3).

Samples from both 5 and 20 min incubations were used for calculating the results. The shorter incubation time might not shave enough surface proteins from the cell surface, while a longer incubation time might result in such small peptides from the mannan core protein to afford too little information for protein identification. The combination of the results from both incubations gave complementary data affording better identification.

Proteins were classified according to the functional categories based on UniProt Gene Ontology (Figure 7B).[36] Most of the proteins identified are involved in transporter function followed by biogenesis, ATP binding, and stress response. Some of these have already been reported in the cell wall of *C. albicans*.[34] Proteins also have been classified according to the locations based on UniProt Gene Ontology (Figure 7C). More than half of the identified proteins were located on the membrane, confirming the robustness of our sample processing and protein identification methods. Some nuclear proteins were identified, but these could be the result of unknown export pathways involved in their secretion. Since *C. auris* proteomics is so poorly studied, some proteins may not yet have been annotated as being located in the cell membrane.

Structural Models of *Candida* Mannan. We combined the possible structures of the four mannans on the basis of our structural analysis of phosphodiesterified oligosaccharides and the resulting acetolysis derived oligosaccharides (Figure 8). These mannans mainly contained four categories of oligosaccharide branches. The first one contains one α-1,3-linkage in α-1,2-linked chains, and the other three contain one, two, or three β-1,2-linkage at the terminal of the α-1,2-linked chains. The molar ratio of different categories of branch oligosaccharides was quantified by the peak area of their specific ^{1}H NMR signals (Figure 1) at around 4.77, 4.85, 4.91, and 5.03 ppm, and these results are shown in Table S4. We ignored the signal contributions of the β-1,2-linkage from phosphodiesterified oligosaccharides, since these were in minimal amounts in these three mannans. The *C. haemulonii* mannan and *C. auris* mannan could be definitively distinguished on the basis of the data presented in Table S2. *C. haemulonii* mannan had reduced amounts of structures with two or three β-1,2-linkages at the terminal of α-1,2-linked chains but more structures containing one α-1,3-linkage in α-1,2-linked chains. From the comparison of ^{1}H NMR signal intensities at 4.89 ppm (Figure 1), specific for the backbone with no side branch structure, -6Manα1-6Manα1-6Manα1-,[28] *C. auris* mannans showed denser side branches than the *C. haemulonii* mannan. Of the two *C. auris* mannans, *C. auris* 17-12 mannan had a higher content of phosphodiesterified oligosaccharides than the *C. auris* 16-4 mannan. However, *C. auris* 16-4 mannan had more one, two, and three β-1,2-linkage structures at terminal α-1,2-linked chains in its acid-stable portion. From the acetolysis studies, the Manβ1-2Manβ1-2Manα1-2Manα1-2Manα was found to be the major oligosaccharide branch in the two *C. auris* mannans. It is noteworthy that *C. lusitaniae*, which is most closely related to *C. auris*, consistent with the percent nucleotide identities of various yeast species,[1] also contains structures of Manβ1-2Manβ1-2Manα1-2Manα1-2Manα as the majority of the branch oligosaccharides in its cell surface mannan.[29] In *C. albicans* mannan, no β-1,2-linkages were found in the acid-stable portion. The Manα1-3Manα1-2Manα1-2Manα1-2Manα and Manα1-3(Manα1-6)Manα1-2Manα1-2Manα1-2Manα were its major branch oligosaccharides. However, its phosphodiesterified oligosaccharides contained only β-1,2-linked mannooligosaccharides. The structure obtained was nearly the same as that published for the *C. albicans* serotype B strain.[30]

The monosaccharide composition of the cell surface glycans from these four *Candida* species was also determined. Their glycans were all mainly made up of glucose and mannose. The ratios of glucose to mannose of glycans from *C. auris* 16-4, *C. auris* 17-12, *C. albicans*, and *C. haemulonii* were 0.68 ± 0.08, 0.60 ± 0.02, 1.50 ± 0.15, and 0.91 ± 0.09, respectively. Moreover, the composition indicates that *C. auris* glycans are richer in cell surface mannans than the other two *Candida* species. On the basis of these analyses, we propose the mannan structure for *C. auris* 16-4 and 17-12, *C. haemulonii*, and *C. albicans* shown in Figure 8.

DISCUSSION

Candida mannans were extracted by enzymatic treatments to preserve their integrity and characterized by NMR spectroscopy using TOCSY to characterize terminal β-1,2-linked mannose units. On the basis of the published reports for other *Candida* species,[15,28−31] we could distinguish unique structures of *C. auris* mannans.

https://dx.doi.org/10.1021/acsinfecdis.9b00450
ACS Infect. Dis. 2020, 6, 1018−1031

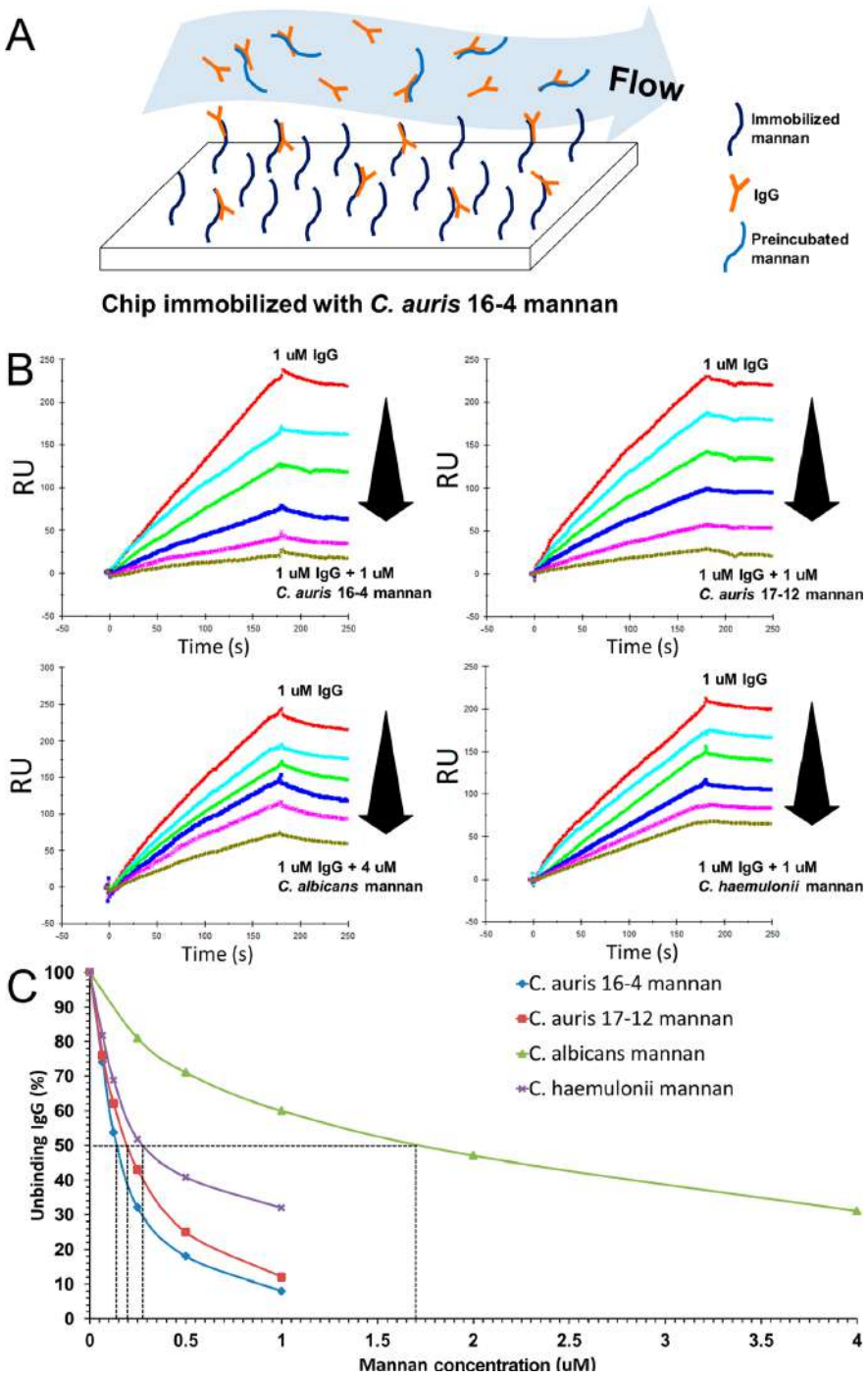

Figure 6. (A) Schematic for mannan-IgG binding competition. (B) Competition of IgG (1 μM) binding to immobilized *C. auris* 16-4 mannan by gradient concentrations of (upper left) *C. auris* 16-4 mannan, (upper right) *C. auris* 17-12 mannan, (lower left) *C. albicans* mannan, and (lower right) *C. haemulonii* mannan with (C) a corresponding IC_{50} value. IgG was preincubated with gradient concentrations of mannans prior to the interaction with immobilized *C. auris* 16-4 mannan. The unbinding IgG was the one that did not interact with the mannan during preincubation. Unbound IgG (%) was calculated by the highest response unit (RU) ratio with and without preincubated mannan.

We used acetolysis to analyze the detailed structures of mannans from *C. auris*, *C. haemulonii*, and *C. albicans* by starting with the phosphodiesterified oligosaccharides. The yields of phosphodiesterified oligosaccharides were consistent with their NMR spectra. The *C. albicans* mannan and *C. auris* 17-12 mannan show intense signals associated with phospho-

https://dx.doi.org/10.1021/acsinfecdis.9b00450
ACS Infect. Dis. 2020, 6, 1018−1031

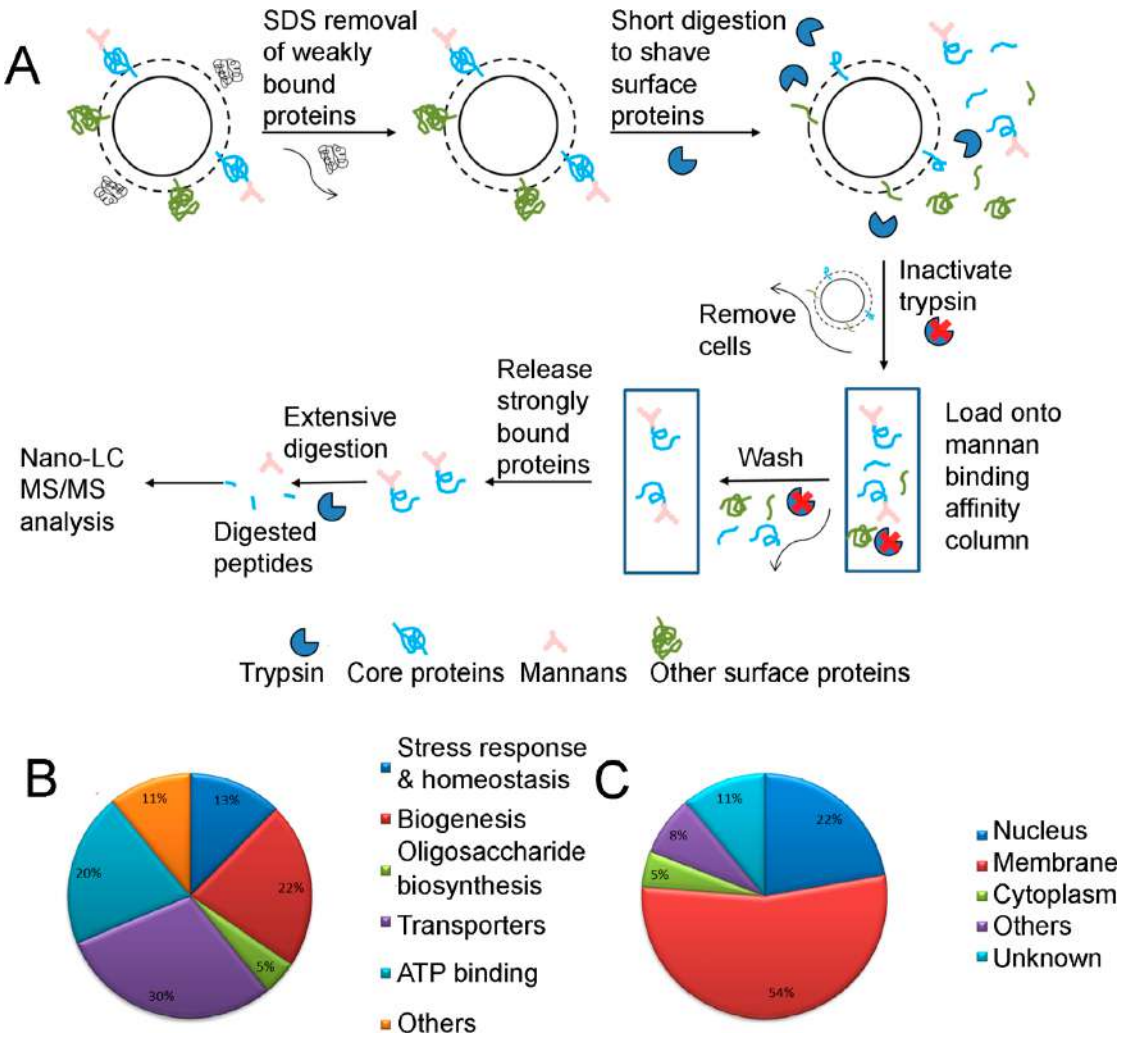

Figure 7. Summary of proteomics analysis of cell-surface mannoproteins from *C. auris*. (A) Approaches for enrichment of cell-surface mannoproteins from *C. auris*. (B) Identified mannoproteins classified by function. (C) Identified mannoproteins classified by location.

diesterified oligosaccharides, while *C. auris* 16-4 mannan and *C. haemulonii* mannan show only weak signals. The structures of phosphodiesterified oligosaccharides from *C. albicans* mannans are consistent with earlier reports about those from the *C. albicans* NIH B-792 (serotype B) strain.[38] However, the structures of phosphodiesterified oligosaccharides from the other three mannans are more similar to the mannans of *C. lusitaniae* and *C. albicans* serotype A.[28,29]

Mild acetolysis was performed on acid-stable mannan to obtain intact, independent branched oligosaccharides, while retaining the labile β-1,2-linked nonreducing terminal groups.[39] The structure of each branched oligosaccharide from *C. albicans* is nearly identical to the previously reported structures of *C. albicans* serotype B.[30] These results confirm the consistency of acetolysis for structural analysis of *Candida* mannans in the present study.

The two *C. auris* mannans and *C. haemulonii* mannans shared the same structural model, since they contained the same linkage types of branch oligosaccharides in the acid-stable portion and phosphodiesterified oligosaccharides. This observation reflects that *C. auris* is phylogenetically related to *C. haemulonii* and that *C. auris* can be easily clinically misidentified as *C. haemulonii*.[26,40] However, the proportions of the branched oligosaccharides were different between *C. auris* mannan and *C. haemulonii* mannan.

Shaved *C. auris* mannoproteins (Figure 7) were used as a control group to increase the identification confidence of *C. auris* cell surface binding proteins from human serum (Table 1). None of the human serum proteins and their unique peptides were found from the *C. auris* control group. There were five proteins identified as *C. auris* surface binding proteins, but only two of these, IgG and MBL, showed strong binding to purified mannan by SPR. Human MBL fused with IgG1 has been reported to bind to *C. auris*.[41,42] MBL is a crucial host-defense protein associated with the innate immune system, and a deficiency of MBL increases susceptibility to many infectious diseases. As a calcium-dependent, pattern-recognition opsonin, MBL can distinguish patterns of carbohydrate molecules associated with the pathogen cell surfaces and subsequently activate the immune system.[41]

https://dx.doi.org/10.1021/acsinfecdis.9b00450
ACS Infect. Dis. 2020, 6, 1018−1031

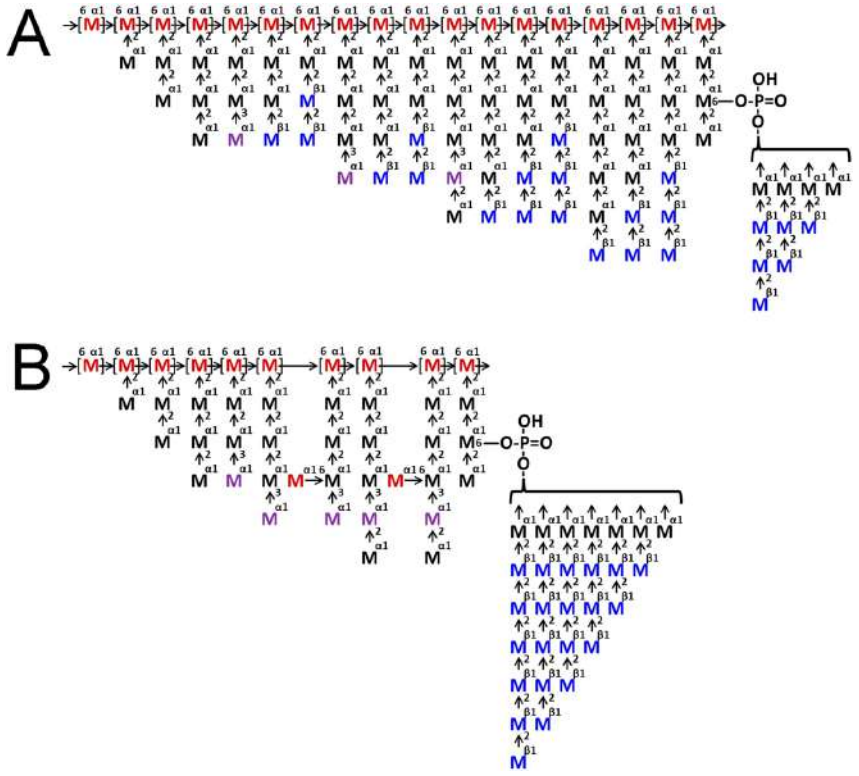

Figure 8. Structural models of *Candida* mannans. (A) *C. auris* 16-4 mannan, *C. auris* 17-12 mannan, and *C. haemulonii* mannan and (B) *C. albicans* mannan. "M" denotes a D-mannopyranose residue. This structure is one of the possibilities out of a statistical ensemble, and there is no specified side-chain order. The M in black corresponds to an α-1,2-linkage. The M in dark red corresponds to an α-1,6-linkage; the M in blue corresponds to a β-1,2-linkage, and the M in purple corresponds to an α-1,3-linkage.

Another protein identified was human immunoglobulin gamma (IgG), which can bind various pathogens, including fungi, to protect the body from infection. One reason for our failure to observe all of the identified binding proteins is that we are examining binding to the purified mannan, not the whole yeast cell. Another reason is that C3 and HRG might instead bind IgG to form a functional complex. In this way, they could indirectly bind to the *C. auris* cell surface through IgG.

Our SPR data suggests that mannans containing a large number of β-1,2-linked mannose residues interact more strongly with IgG and MBL protein. This result is consistent with the previous report that *Candida* mannan in candidiasis patients contains β-1,2-linked mannose residues, and these are targets of the immune system.[28] Also, an earlier publication describes that glycopeptide vaccines combining β-mannan and peptide epitopes induce protection against candidiasis in a murine model.[42] *C. auris* may rely on a surface mannan rich in β-1,2-linkages to interact with immune proteins like IgG and MBL. Further studies are needed to examine if the *C. auris* β-1,2-linkage is critical for interactions with the immune system.

In conclusion, studies on the glycomics and proteomics of *C. auris* led to the discovery of a unique mannan. *Candida auris* mannan is distinct from closely and distantly related pathogenic *Candida* species. *Candida auris* mannan mainly resides on the surface of yeast. *C. auris* mannan could be crucial for the biology and pathogenesis of this emerging pathogen.

MATERIALS AND METHODS

Materials. Lyticase and amyloglucosidase were purchased from Sigma-Aldrich (St. Louis, MO, USA). β-Glucosidase was purchased from Megazyme (Bray, Ireland). Centrifugal filter units of 10K molecular weight cutoff (MWCO) were purchased from MilliporeSigma (Burlington, MA, USA). Centrifugal filter units of 0.2 μm were purchased from Pall (Port Washington, NY, USA). Human serum was purchased from BIOVIT (Westbury, NY, USA). Pierce mannan binding protein agarose was purchased from Thermo Fisher Scientific (Waltham, MA, USA). Tryspsin gold was purchased from Promega (Madison, WI, USA). All other chemicals and reagents were of analytical grade and purchased from commercial corporations.

Preparation and Inactivation of *Candida*. *Candida auris* (16-4 and 17-12, South Asian clade), *C. albicans*, and *C. haemulonii* were clinical isolates characterized by MALDI-TOF-MS (matrix-assisted laser desorption/ionization time-of-flight mass spectrometry) and Sanger sequencing at the Mycology Laboratory, Wadsworth Center.[9] The South Asian Clade I predominates among patients in New York.[9] Bulk preparations were obtained from yeast cells grown for 24 h in yeast extract-peptone (YPD) broth at 30 °C and 180 rpm. Cell pellets were obtained by centrifugation and heat-inactivated in a water bath (90 °C, 180 min) or autoclave (121 °C, 30 min). The sterility of the heat-inactivated cells was checked by transferring a 10 μL loop full of pellet to 20 mL of YPD broth incubated at 30 °C and 180 rpm for 48 h.

https://dx.doi.org/10.1021/acsinfecdis.9b00450
ACS Infect. Dis. 2020, 6, 1018−1031

Preparation of Mannan. Autoclaved or heat-inactivated *Candida* strains were lyophilized, and then, each milligram of dry *Candida* strain was mixed with 50 to 100 active units of lyticase and 0.1 to 0.2 mL of pure water at room temperature overnight. The precipitate was removed by centrifugation; the supernatant was recovered, and the impurities from enzymatic hydrolysis were removed using a 10K MWCO centrifugal filter unit allowing for the recovery of the intact glycoprotein from the cell surface. After lyophilization, each milligram of dry glycoprotein was mixed with one active unit of amyloglucosidase and 0.1 to 0.2 mL of 50 mM sodium acetate-HCl (pH 4.70) and incubated at 55 °C overnight to remove α-glucans. Next, each milligram of dry glycoprotein was mixed with one active unit of β-glucosidase and 0.1 to 0.2 mL of 50 mM sodium phosphate (pH 7.00) and incubated at 40 °C overnight to remove β-glucans. ^{1}H NMR spectroscopy was used to make sure all the glucans were removed from the glycoprotein (data were not shown). Next, each milligram of mannoprotein was mixed with 0.1 mg of actinase E and 0.1 mL of pure water and incubated at 55 °C overnight to digest the protein part. Finally, after treatment at 100 °C for 1 h, the actinase E was removed by centrifugation and the pure mannan was enriched by a 10K MWCO centrifugal filter unit and then lyophilized to obtain a final yield of ∼5% based on the starting dry cell weight.

Acetolysis of the Mannan. Before acetolysis, the mannan was treated with 10 mM HCl at 100 °C for 1 h to release the phosphodiesterified oligosaccharides. Then, 100 mg of acid-stable mannan was acetylated in 20 mL of a mixture of acetic anhydride/pyridine (1:1 by vol.) at 105 °C in an oil bath for 24 h, after which, rotary evaporation was used to remove anhydride and pyridine. The acetylated mannan was dissolved in 20 mL of a mixture of acetic anhydride/acetic acid/H_2SO_4 (100:100:1 by vol.) at 40 °C for 36 h as mild acetolysis. Next, 40 mL of pyridine was added to stop the acetolysis, and rotary evaporation was used to dry the sample. The acetylated oligosaccharides were extracted by chloroform and then deacetylated using sodium methoxide. Finally, the mixture was deionized by dialysis and then freeze-dried. This treatment selectively breaks the backbone α-1,6-linkages of acid-stable mannan and yields a mixture of oligosaccharides from side-chain moieties.

HPGPC and HPLC of Oligosaccharides. HPGPC of oligosaccharides was profiled on a column (10 × 300 mm) of Superdex Peptide 10/300 GL (GE Healthcare, Chicago, IL). Elution was carried out with 0.2 M NH_4HCO_3 at a flow rate of 0.4 mL/min and was monitored with a refractive index detector. High performance liquid chromatography (HPLC) of oligosaccharides was profiled on a column (4.6 mm × 250 mm) of YMC-Pack PA-G (YMC American, Allentown, PA, USA). Elution was carried out with CH_3CN/H_2O (52:48, v/v) at a flow rate 1.0 mL/min and was monitored with a refractive index detector.

NMR Spectroscopy. Samples were dissolved in 500 μL of D_2O (99.9%) and lyophilized three times to substitute the exchangeable protons with deuterium and then transferred to NMR microtubes after dissolving in 500 μL of D_2O. NMR spectra were recorded on Bruker 600 spectrometer (Madison, WI, USA) with Topspin 3.2 software at 318.15 K.

Monosaccharide Composition of Cell Surface Glycans. Autoclaved or heat-inactivated *Candida* strains were treated with a protease, actinase E, to recover glycans from the cell surface. The monosaccharide composition of cell surface glycans was determined by the 1-phenyl-3-methyl-5-pyrazolone (PMP) derivatization followed by HPLC as mentioned in a similar publication.[43] Briefly, cell surface glycans were hydrolyzed with 2 M trifluoroacetic acid (TFA) at 110 °C for 8 h. The hydrolyzate was derived in a methanol solution of PMP at 70 °C for 30 min. The labeled carbohydrates were analyzed by HPLC with a mixture of 0.1 M KH_2PO_4 and CH_3CN (83:17, v/v) as mobile phase. D-Glucose, L-rhamnose, D-xylose, L-arabinose, D-mannose, L-fucose, D-galactose, and D-galacturonic acid were derived and used as standards.

Interaction Studies between *Candida* Mannans and Serum Proteins. The interaction behavior of *Candida* mannans with serum proteins was measured using SPR on a BIAcore 3000 system based on a similar publication.[44] Briefly, the biotinylated *Candida* mannan was immobilized to a streptavidin (SA) chip based on the manufacturer's protocol. Successful immobilization of *Candida* mannan was confirmed by the observation of an over 400 resonance unit (RU) increase in the sensor chip. The commercial serum protein was resuspended in PBS buffer. Different dilutions of the serum protein were injected at a flow rate of 30 μL/min. At the end of the injection, the same buffer was flowed over the sensor surface to facilitate dissociation. After dissociation, the sensor surface was regenerated by injecting 30 μL of 2 M NaCl. The response was monitored as a function of time (sensorgram) at 25 °C.

Competition of IgG Binding to Immobilized *C. auris* 16-4 Mannan by Different *Candida* Mannans. Competitive SPR experiments, using different *Candida* mannans, were performed to compare their binding ability to IgG. IgG was separately preincubated with a gradient of concentrations of different *Candida* mannans and then injected over the *C. auris* 16-4 mannan chip at a flow rate of 30 μL/min. After each injection and association, dissociation and regeneration were performed as previously described.

Isolation of Mannoproteins for Proteomics. A cell shaving method was used to identify the core protein of the surface mannoprotein.[34,35] Briefly, *C. auris* cells heat-inactivated at 90 °C were collected and washed four times in 1% sodium dodecyl sulfate (SDS) to remove proteins weakly bound to the cell surface. The intact nature of the cells was verified by microscopy to confirm that the SDS did not break the cells and released proteins primarily from the cell surface (Figure S4). Cells were then resuspended in 0.8 mL of 25 mM ammonium bicarbonate buffer (pH 8.0). A total amount of 10 μg of trypsin (Trypsin Gold, Promega) was added to 10 mg cells. Since unfolded proteins are more accessible to tryptic digestion, the efficiency of surface digestion was enhanced in the presence of 0.5 mM DTT. After incubation at 37 °C for 5 min in a rotary shaker at 600 rpm, proteolytic reactions were first stopped by adding 0.1% TFA (v/v) followed by heating for 10 min at 98 °C to permanently deactivate the trypsin. Samples were centrifuged at 3500*g* for 5 min, and the supernatants were collected and filtered through 0.22 μm pore-size filters (Pall, NY, USA). The intact nature of the cells was again verified by microscopy to make certain that trypsin digestion did not break the cells and that the proteins released were primarily from the cell surface (Figure S4).

Purification of Shaved Mannoproteins. The affinity column was carefully packed with the immobilized MBP (Pierce) according to the manufacturer's instructions. The column was equilibrated at 4 °C by washing with eight gel-bed volumes of prechilled binding buffer (10 mM Tris, 1.25 M

https://dx.doi.org/10.1021/acsinfecdis.9b00450
ACS Infect. Dis. 2020, 6, 1018−1031

NaCl, 20 mM $CaCl_2$; pH 7.4; 4 °C). Cold (4 °C) shaved mannoprotein samples were added to the column and allowed to completely enter the gel. Next, 2 mL of binding buffer per 5 mL of gel bed was added to the column and incubated at 4 °C for 30 min. The washed column was loaded with nine gel-bed volumes of the cold binding buffer to remove nonbound protein. The elution procedure was performed at room temperature by adding 3 mL of elution buffer to the column for each 5 mL of gel. After overnight incubation, shaved mannoprotein fractions were collected by adding nine gel-bed volumes of the elution buffer.

Identification of *C. auris* Cell Surface Binding Proteins from Human Serum. Human serum was from a pool of healthy donor volunteers who did not have any clinical or microbiological evidence of infection (BIOVIT). Human serum (1 mL) was added to 9 mL of phosphate buffered saline (PBS) (10 mM). Glutaraldehyde (10 mg) was used to treat *C. auris* and was gently mixed with the dilute serum and then incubated 5 h at 37 °C and 200 rpm. Two *C. auris* strains were incubated, and each incubation was performed in duplicate.

The surface shaving procedure was adapted from a previous study.[35] Briefly, after incubation of *C. auris* with 10% human serum, the cultures were centrifuged at 3500*g* for 5 min. Cell pellets were resuspended in 1 mL of PBS with 0.1% Tween 20, centrifuged again, and washed 6 times with PBS to remove nonspecific, weak-bonding proteins. The washed pellet was resuspended in 400 μL of 25 mM NH_4HCO_3, pH 8.0. Next, 7.5 μL of 1 M dithiothreitol (DTT) and 9 μg of trypsin gold (Promega) were added. DTT was added during the digestion as a reducing agent to ensure deep digestion of the associated proteins with noncovalent and disulfide bridges. In contrast to the experiment aimed at shaving mannoproteins from the cell surface without extensive digestion, this process aims to fully digest human serum proteins that are strongly bonded to the cell surface. Therefore, samples are incubated for a longer time (30 min) at 37 °C and 600 rpm. After incubation, TFA 0.1% (v/v) was added to stop the proteolytic reaction; samples were centrifuged at 5000 rpm for 5 min, and the supernatant was filtered with a centrifugal filter unit of 10K MWCO to remove trypsin, mannan, and cells. The samples were freeze-dried and stored at −20 °C before nano-LC-MS/MS analysis.

Nano HPLC MS/MS. The resulting peptide mixtures were analyzed using an Agilent 1200-Series LC system coupled to an LTQ-Orbitrap mass spectrometer (Thermo Fisher Scientific, Waltham, MA USA). The LC system was equipped with a 75 μm ID, 15 μm tip, 105 mm picochip (New Objective, Cambridge, MA) bed packed with 5 μm BioBasic (Thermo Fisher Scientific, Waltham, MA USA) C18 and 300 Å resin. Sample loading was finished in 2% buffer B (98% acetonitrile in 0.1% formic acid) in 10 min. Elution was achieved with a gradient of 15−90% B in a total of 180 min. The flow rate was passively split from 0.3 mL/min to 200 nL/min. The mass spectrometer was operated in data-dependent mode to switch between MS and MS/MS. The five most intense ions were selected for fragmentation in the linear ion trap using collision-induced dissociation. For each sample, MS/MS tests have been repeated several times.

MS Data Analysis. Mass spectrometry data were analyzed using the Trans-Proteomic Pipeline (TPP) Version 5.2.0. TPP-processed centroid fragment peak lists in mzML format were searched against a corresponding reference database composed of *C. auris* proteins (Uniprot) or *Homo sapiens* (Uniprot). The database searches were performed using Comet through the TPP. Search parameters included: trypsin cleavage specificity with two missed cleavages, methionine oxidation, peptide tolerance, and MS/MS tolerance at 20 ppm. Peptide lists from two repeated tests were combined in IPROPHET. Peptide and protein lists were generated following Peptide Prophet and Protein Prophet analysis using a protein FDR of 1%. When searching for proteins in Unitprot, UnitProt GO provides a GO subcellular location for the identified proteins. For example, the protein at the top of Table S3, A0A2H0ZW65 MFS domain-containing protein, is given a location labeled as an integral component of the membrane [GO:0016021]. When no direct assignment is given to an uncharacterized protein, the most homologous protein predicted by Pannzer2 is used to assign the location. However, since the proteomic database and annotations for *C. auris* are far from complete, some uncharacterized proteins do not have close homology to any other proteins and the location assignment is listed as unknown (see Figure 7C).

■ ASSOCIATED CONTENT

Supporting Information

The Supporting Information is available free of charge at https://pubs.acs.org/doi/10.1021/acsinfecdis.9b00450.

Proton chemical shifts; proteins with predicted functions identified from surface mannoproteins; molar ratio of different categories of branch oligosaccharides; HPGPC profiles; correspondence between HPGPC by Superdex Peptide 10/300 GL column and HPLC by YMC Pack PA-G column profiles; SPR sensorgrams; intact nature of the cells (PDF)

■ AUTHOR INFORMATION

Corresponding Authors

Vishnu Chaturvedi − *Mycology Laboratory, Wadsworth Center, New York State Department of Health, Albany, New York 12201, United States; Department of Biomedical Sciences, University at Albany School of Public Health, Albany, New York 12222, United States;* orcid.org/0000-0002-3922-9676; Email: vishnu.chaturvedi@health.ny.gov

Robert J. Linhardt − *Center for Biotechnology & Interdisciplinary Studies and Department of Chemistry & Chemical Biology, Rensselaer Polytechnic Institute, Troy, New York 12180, United States;* orcid.org/0000-0003-2219-5833; Email: linhar@rpi.edu

Authors

Lufeng Yan − *Center for Biotechnology & Interdisciplinary Studies and Department of Chemistry & Chemical Biology, Rensselaer Polytechnic Institute, Troy, New York 12180, United States;* orcid.org/0000-0002-6772-4615

Ke Xia − *Center for Biotechnology & Interdisciplinary Studies and Department of Chemistry & Chemical Biology, Rensselaer Polytechnic Institute, Troy, New York 12180, United States;* orcid.org/0000-0001-9699-9901

Yanlei Yu − *Center for Biotechnology & Interdisciplinary Studies and Department of Chemistry & Chemical Biology, Rensselaer Polytechnic Institute, Troy, New York 12180, United States;* orcid.org/0000-0002-2736-8644

Anna Miliakos − *Center for Biotechnology & Interdisciplinary Studies and Department of Chemistry & Chemical Biology, Rensselaer Polytechnic Institute, Troy, New York 12180, United States;* orcid.org/0000-0001-8838-7462

https://dx.doi.org/10.1021/acsinfecdis.9b00450
ACS Infect. Dis. 2020, 6, 1018−1031

Sudha Chaturvedi − *Mycology Laboratory, Wadsworth Center, New York State Department of Health, Albany, New York 12201, United States; Department of Biomedical Sciences, University at Albany School of Public Health, Albany, New York 12222, United States;* orcid.org/0000-0003-0906-8426

Fuming Zhang − *Center for Biotechnology & Interdisciplinary Studies and Department of Chemistry & Chemical Biology, Rensselaer Polytechnic Institute, Troy, New York 12180, United States;* orcid.org/0000-0003-2803-3704

Shiguo Chen − *Center for Biotechnology & Interdisciplinary Studies and Department of Chemistry & Chemical Biology, Rensselaer Polytechnic Institute, Troy, New York 12180, United States;* orcid.org/0000-0002-6439-7735

Complete contact information is available at: https://pubs.acs.org/10.1021/acsinfecdis.9b00450

Author Contributions

#L.Y. and K.X. contributed equally.

Notes

The authors declare no competing financial interest.

■ ACKNOWLEDGMENTS

The authors acknowledge support from the NIH in the form of grants DK111958 and CA231074 [R.J.L.]. The study was also supported in part with internal funds from Wadsworth Center, New York State Department of Health [V.C.].

■ REFERENCES

(1) Satoh, K., Makimura, K., Hasumi, Y., Nishiyama, Y., Uchida, K., and Yamaguchi, H. (2009) *Candida auris* sp. nov., a novel ascomycetous yeast isolated from the external ear canal of an inpatient in a Japanese hospital. *Microbiol. Immunol. 53*, 41−44.

(2) Lockhart, S. R., Etienne, K. A., Vallabhaneni, S., Farooqi, J., Chowdhary, A., Govender, N. P., Colombo, A. L., Calvo, B., Cuomo, C. A., Desjardins, C. A., et al. (2017) Simultaneous emergence of multidrug-resistant *Candida auris* on 3 continents confirmed by whole-genome sequencing and epidemiological analyses. *Clin. Infect. Dis. 64*, 134−140.

(3) Muñoz, J. F., Gade, L., Chow, N. A., Loparev, V. N., Juieng, P., Berkow, E. L., Farrer, R. A., Litvintseva, A. P., and Cuomo, C. A. (2018) Genomic insights into multidrug-resistance, mating and virulence in *Candida auris* and related emerging species. *Nat. Commun. 9*, 5346.

(4) Ostrowsky, B., Greenko, J., Adams, E., Quinn, M., O'Brien, B., Chaturvedi, V., Berkow, E., Vallbhaneni, S., Forsberg, K., Chaturvedi, S., Lutterloh, E., Blog, D., and *C. auris* Investigation Work Group (2020) Candida auris isolates resistant to three classes of antifungal medications — New York, 2019. *Morb. Mortal. Wkly. Rep. 69* (1), 6−9.

(5) Montoya, M. C., Moye-Rowley, W. S., and Krysan, D. J. (2019) *Candida auris*: The canary in the mine of antifungal drug resistance. *ACS Infect. Dis. 5*, 1487−1492.

(6) Schelenz, S., Hagen, F., Rhodes, J. L., Abdolrasouli, A., Chowdhary, A., Hall, A., Ryan, L., Shackleton, J., Trimlett, R., Meis, J. F., Armstrong-James, D., and Fisher, M. C. (2016) First hospital outbreak of the globally emerging *Candida auris* in a European hospital. *Antimicrob. Resist. Infect. Control. 5*, 35.

(7) Adams, E, Quinn, M, Tsay, S, Poirot, E, Chaturvedi, S, Southwick, K, Greenko, J, Fernandez, R, Kallen, A, Vallabhaneni, S, Haley, V, Hutton, B, Blog, D, Lutterloh, E, Zucker, H, and *Candida auris* Investigation Workgroup (2018) Candida auris in Healthcare Facilities, New York, USA, 2013−2017. *Emerging Infect. Dis. 24* (10), 1816−1824.

(8) de Jong, A. W., and Hagen, F. (2019) Attack, defend, persist: How the fungal pathogen *Candida auris* was able to emerge globally in health care environments. *Mycopathologia 184* (3), 353−365.

(9) Zhu, Y., O'Brien, B., Leach, L., Clark, A., Bates, M., Adams, E., Ostrowsky, B., Quinn, M., Dufort, E., Southwick, K., Erazo, R., Haley, V. B., Bucher, C., Chaturvedi, V., Limberger, R. J., Blog, D., Lutterloh, E., and Chaturvedi, S. (2020) Laboratory analysis of an outbreak of *Candida auris* in New York from 2016 to 2018-Impact and lessons learned. *J. Clin. Microbiol. 58*, e01503-19.

(10) Kenters, N., Kiernan, M., Chowdhary, A., Denning, D. W., Pemán, J., Saris, K., Schelenz, S., Tartari, E., Widmer, A., Meis, J. F., and Voss, A. (2019) Control of *Candida auris* in healthcare institutions: Outcome of an International Society for Antimicrobial Chemotherapy expert meeting. *Int. J. Antimicrob. Agents 54* (4), 400−406.

(11) Tsay, S., Kallen, A., Jackson, B. R., Chiller, T. M., and Vallabhaneni, S. (2018) Approach to the investigation and management of patients with *Candida auris*, an emerging multidrug-resistant yeast. *Clin. Infect. Dis. 66* (2), 306−311.

(12) Chatterjee, S., Alampalli, S. V., Nageshan, R. K., Chettiar, S. T., Joshi, S., and Tatu, U. S. (2015) Draft genome of a commonly misdiagnosed multidrug resistant pathogen *Candida auris*. *BMC Genomics 16*, 686.

(13) Eyre, D. W., Sheppard, A. E., Madder, H., Moir, I., Moroney, R., Quan, T. P., Griffiths, D., George, S., Butcher, L., Morgan, M., Newnham, R., Sunderland, M., Clarke, T., Foster, D., Hoffman, P., Borman, A. M., Johnson, E. M., Moore, G., Brown, C. S., Walker, A. S., Peto, T. E. A., Crook, D. W., and Jeffery, K. J. M. (2018) A *Candida auris* outbreak and its control in an intensive care setting. *N. Engl. J. Med. 379*, 1322−1331.

(14) Chaffin, W. L., López-Ribot, J. L., Casanova, M., Gozalbo, D., and Martínez, J. P. (1998) Cell wall and secreted proteins of *Candida albicans*: identification, function, and expression. *Microbiol. Mol. Biol. Rev. 62* (1), 130−180.

(15) Shibata, N., Kobayashi, H., and Suzuki, S. (2012) Immunochemistry of pathogenic yeast, *Candida* species, focusing on mannan. *Proc. Jpn. Acad., Ser. B 88* (6), 250−265.

(16) Cambi, A., Netea, M. G., Mora-Montes, H. M., Gow, N. A., Hato, S. V., Lowman, D. W., Kullberg, B. J., Torensma, R., Williams, D. L., and Figdor, C. G. (2008) Dendritic cell interaction with *Candida albicans* critically depends on N-linked mannan. *J. Biol. Chem. 283* (29), 20590−20599.

(17) Tronchin, G., Pihet, M., Lopes-Bezerra, L. M., and Bouchara, J. P. (2008) Adherence mechanisms in human pathogenic fungi. *Med. Mycol. 46* (8), 749−772.

(18) Willaert, R. G. (2018) Adhesins of yeasts: Protein structure and interactions. *J. Fungi 4* (4), 119.

(19) Miyakawa, Y., Kuribayashi, T., Kagaya, K., Suzuki, M., Nakase, T., and Fukazawa, Y. (1992) Role of specific determinants in mannan of *Candida albicans* serotype A in adherence to human buccal epithelial cells. *Infect. Immun. 60* (6), 2493−2499.

(20) Maestre-Reyna, M., Diderrich, R., Veelders, M. S., Eulenburg, G., Kalugin, V., Brückner, S., Keller, P., Rupp, S., Mösch, H. U., and Essen, L. O. (2012) Structural basis for promiscuity and specificity during *Candida glabrata* invasion of host epithelia. *Proc. Natl. Acad. Sci. U. S. A. 109* (42), 16864−16869.

(21) Diderrich, R., Kock, M., Maestre-Reyna, M., Keller, P., Steuber, H., Rupp, S., Essen, L. O., and Mösch, H. U. (2015) Structural hot spots determine functional diversity of the *Candida glabrata* epithelial adhesin family. *J. Biol. Chem. 290* (32), 19597−19613.

(22) Ruiz-Herrera, J., Elorza, M. V., Valentín, E., and Sentandreu, R. (2006) Molecular organization of the cell wall of *Candida albicans* and its relation to pathogenicity. *FEMS Yeast Res. 6* (1), 14−29.

(23) Mencacci, A., Torosantucci, A., Spaccapelo, R., Romani, L., Bistoni, F., and Cassone, A. (1994) A mannoprotein constituent of *Candida albicans* that elicits different levels of delayed-type hypersensitivity, cytokine production, and anticandidal protection in mice. *Infect. Immun. 62* (12), 5353−60.

(24) Lipinski, T., Wu, X., Sadowska, J., Kreiter, E., Yasui, Y., Cheriaparambil, S., Rennie, R., and Bundle, D. R. (2012) A β-mannan trisaccharide conjugate vaccine aids clearance of *Candida albicans* in immunocompromised rabbits. *Vaccine 30* (44), 6263−6269.
(25) Paulovičová, E., Paulovičová, L., Farkaš, P., Karelin, A. A., Tsvetkov, Y. E., Krylov, V. B., and Nifantiev, N. E. (2019) Importance of *Candida* antigenic factors: structure-driven immunomodulation properties of synthetically prepared mannooligosaccharides in RAW264.7 macrophages. *Front. Cell. Infect. Microbiol. 9*, 378.
(26) Weiner, M. H., and Yount, W. J. (1976) Mannan antigenemia in the diagnosis of invasive *Candida* infections. *J. Clin. Invest. 58* (5), 1045−53.
(27) Sendid, B., Poirot, J. L., Tabouret, M., Bonnin, A., Caillot, D., Camus, D., and Poulain, D. (2002) Combined detection of mannanaemia and antimannan antibodies as a strategy for the diagnosis of systemic infection caused by pathogenic *Candida* species. *J. Med. Microbiol. 51* (5), 433−42.
(28) Shibata, N., Suzuki, A., Kobayashi, H., and Okawa, Y. (2007) Chemical structure of the cell-wall mannan of *Candida albicans* serotype A and its difference in yeast and hyphal forms. *Biochem. J. 404*, 365−372.
(29) Shibata, N., Kobayashi, H., Okawa, Y., and Suzuki, S. (2003) Existence of novel beta-1,2 linkage-containing side chain in the mannan of *Candida lusitaniae*, antigenically related to *Candida albicans* serotype A. *Eur. J. Biochem. 270* (12), 2565−2575.
(30) Shibata, N., Ikuta, K., Imai, T., Satoh, Y., Satoh, R., Suzuki, A., Kojima, C., Kobayashi, H., Hisamichi, K., and Suzuki, S. (1995) Existence of branched side-chains in the cell-wall mannan of pathogenic yeast, *Candida albicans* - Structure-antigenicity relationship between the cell-wall mannans of *Candida albicans* and *Candida parapsilosis*. *J. Biol. Chem. 270* (3), 1113−1122.
(31) Shibata, N., Akagi, R., Hosoya, T., Kawahara, K., Suzuki, A., Ikuta, K., Kobayashi, H., Hisamichi, K., Okawa, Y., and Suzuki, S. (1996) Existence of novel branched side chains containing beta-1,2 and alpha-1,6 linkages corresponding to antigenic factor 9 in the mannan of *Candida guilliermondii*. *J. Biol. Chem. 271* (16), 9259−9266.
(32) Vidarsson, G., Dekkers, G., and Rispens, T. (2014) IgG subclasses and allotypes: from structure to effector functions. *Front. Immunol. 5*, 520.
(33) Turner, M. W. (2003) The role of mannose-binding lectin in health and disease. *Mol. Immunol. 40* (7), 423−429.
(34) Hernáez, M. L., Ximénez-Embún, P., Martínez-Gomariz, M., Gutiérrez-Blázquez, M. D., Nombela, C., and Gil, C. (2010) Identification of *Candida albicans* exposed surface proteins in vivo by a rapid proteomic approach. *J. Proteomics 73* (7), 1404−1409.
(35) Gil-Bona, A., Parra-Giraldo, C. M., Hernaez, M. L., Reales-Calderon, J. A., Solis, N. V., Filler, S. G., Monteoliva, L., and Gil, C. (2015) *Candida albicans* cell shaving uncovers new proteins involved in cell wall integrity, yeast to hypha transition, stress response and host-pathogen interaction. *J. Proteomics 127*, 340−351.
(36) UniProt Consortium (2019) UniProt: a worldwide hub of protein knowledge. *Nucleic Acids Res. 47* (D1), D506−D515.
(37) Törönen, P., Medlar, A., and Holm, L. (2018) PANNZER2: a rapid functional annotation web server. *Nucleic Acids Res. 46* (W1), W84−W88.
(38) Shibata, N., Hisamichi, K., Kikuchi, T., Kobayashi, H., Okawa, Y., and Suzuki, S. (1992) Sequential nuclear-magnetic-resonance assignment of beta-1,2-Linked mannooligosaccharides isolated from the phosphomannan of the pathogenic yeast *Candida albicans* NIH B-792 strain. *Biochemistry 31* (24), 5680−5686.
(39) Kobayashi, H., Shibata, N., and Suzuki, S. (1986) Acetolysis of *Pichiapastoris*-Ifo-0948 strain mannan containing alpha-1,2 and beta-1,2 linkages using acetolysis medium of low sulfuric-acid concentration. *Arch. Biochem. Biophys. 245* (2), 494−503.
(40) Kathuria, S., Singh, P. K., Sharma, C., Prakash, A., Masih, A., Kumar, A., Meis, J. F., and Chowdhary, A. (2015) Multidrug-resistant *Candida auris* misidentified as *Candida haemulonii*: Characterization by matrix-assisted laser desorption ionization−time of flight mass spectrometry and DNA sequencing and its antifungal susceptibility profile variability by Vitek 2, CLSI broth microdilution, and Etest method. *J. Clin. Microbiol. 53* (6), 1823−1830.
(41) Seiler, B. T., Cartwright, M., Dinis, A. L. M., Duffy, S., Lombardo, P., Cartwright, D., Super, E. H., Lanzaro, J., Dugas, K., Super, M., and Ingber, D. E. (2019) Broad-spectrum capture of clinical pathogens using engineered Fc-mannose-binding lectin enhanced by antibiotic treatment. *F1000Research 8*, 108−108.
(42) Xin, H., Dziadek, S., Bundle, D. R., and Cutler, J. E. (2008) Synthetic glycopeptide vaccines combining beta-mannan and peptide epitopes induce protection against candidiasis. *Proc. Natl. Acad. Sci. U. S. A. 105* (36), 13526−13531.
(43) Yan, L. F., Li, J. H., Wang, D. L., Ding, T., Hu, Y. Q., Ye, X. Q., Linhardt, R. J., and Chen, S. G. (2017) Molecular size is important for the safety and selective inhibition of intrinsic factor Xase for fucosylated chondroitin sulfate. *Carbohydr. Polym. 178*, 180−189.
(44) Zhao, J., Huvent, I., Lippens, G., Eliezer, D., Zhang, A. Q., Li, Q. H., Tessier, P., Linhardt, R. J., Zhang, F. M., and Wang, C. Y. (2017) Glycan determinants of heparin-Tau interaction. *Biophys. J. 112* (5), 921−932.

https://dx.doi.org/10.1021/acsinfecdis.9b00450
ACS Infect. Dis. 2020, 6, 1018−1031